

# A Transformer Framework for Data Fusion and Multi-Task Learning in Smart Cities

Alexander C. DeRieux<sup>1</sup>, Graduate Student Member, IEEE, Walid Saad<sup>2</sup>, Fellow, IEEE, Wangda Zuo<sup>3</sup>, Rachmawan Budiarto<sup>4</sup>, Mochamad Donny Koerniawan<sup>5</sup>, and Dwi Novitasari<sup>6</sup>

**Abstract**—Rapid global urbanization is a double-edged sword, heralding promises of economical prosperity and public health while also posing unique environmental and humanitarian challenges. Smart and connected communities (S&CCs) apply data-centric solutions to these problems by integrating artificial intelligence (AI) and the Internet of Things (IoT). This coupling of intelligent technologies also poses interesting system design challenges regarding heterogeneous data fusion and task diversity. Transformers are of particular interest to address these problems, given their success across diverse fields of natural language processing (NLP), computer vision, time-series regression, and multi-modal data fusion. This begs the question whether Transformers can be further diversified to leverage fusions of IoT data sources for heterogeneous multi-task learning in S&CC trade spaces. In this paper, a Transformer-based AI system for emerging smart cities is proposed. Designed using a pure encoder backbone, and further customized through interchangeable input embedding and output task heads, the system supports virtually any input data and output task types present S&CCs. This generalizability is demonstrated through learning diverse task sets representative of S&CC environments, including multivariate time-series regression, visual plant disease classification, and image-time-series fusion tasks using a combination of Beijing PM2.5 and Plant Village datasets. Simulation results show that the proposed Transformer-based system can handle various input data types via custom sequence embedding techniques, and are naturally suited to learning a diverse set of tasks. The results also show that multi-task learners increase both memory and computational efficiency while maintaining comparable performance to both single-task variants, and non-Transformer baselines.

**Index Terms**—Artificial Intelligence, Multi-Task Learning, Data Fusion, Transformers, Smart Cities, Internet of Things

## I. INTRODUCTION

IT is projected that by 2050 nearly 68% of the global populace will live in urban areas [1]. Rapid urbanization in many countries around the world is ushered by promises of economical prosperity and increased population health

and wellness. However, these boons pose equal challenges pertaining to environmental quality and food cultivation, both of which are vital to sustaining positive growth. Parallel to this expansion is also an increased emphasis on integrating intelligent technologies to build smart and connected communities (S&CCs). Sparked by recent advancements in artificial intelligence (AI) and the Internet of Things (IoT), this convergence of technology and society is the epicenter of S&CC development. In particular, the coupling of AI with IoT poses interesting system design challenges pertaining to data collection, and, most importantly, *data fusion*. Specifically, the question of how to design intelligent systems that can leverage a fusion of heterogeneous features arises. This is critical for data-rich locales, such as S&CC, in which many of the environmental features are captured by IoT, but remain untapped by AI to learn correlations. Hence, next-generation AI systems for S&CC environments must be designed to leverage a fusion of heterogeneous data sources to learn multiple tasks concurrently.

Focusing on the perspective of AI, there have been many interesting architectural developments to learn from sequence-based information. Specifically, Transformers [2] have revolutionized natural language processing (NLP) and neural machine translation (NMT) trade spaces over competitive recurrent neural networks (RNNs) models (i.e., long short-term memory (LSTM), gated recurrent unit (GRU), etc.). Moreover, their affinity for sequence-modeling tasks has also been shown to be applicable in fields of time-series regression [3–7], computer vision [8–10], and multi-modal data fusion [11, 12]. This applicability across many diverse trade spaces begs the question whether attention-based architectures can be further extended to leverage fusions of IoT data sources for heterogeneous multi-task learning in S&CC trade spaces.

### A. Related Works and their Limitations

There has been a recent influx of literature studying the application of Transformers to time-series forecasting [3–7, 13], computer vision [8–10, 14], and multi-modal data fusion [11, 12] trade spaces. In terms of time-series forecasting, the authors of [3] propose the so-called Temporal Fusion Transformer (TFT), which combines LSTM technology with attention mechanisms to make quantile forecasts across multiple time horizons. In [5], the authors propose the first time-series Transformer design consisting of both encoder and decoder blocks to forecast *univariate* temporal data. In [4], the authors propose the Informer architecture, which

This work was funded by the National Science Foundation under Grants CNS-2025377 and CNS-2241361.

A. C. DeRieux and W. Saad are with Wireless@VT, Bradley Department of Electrical and Computer Engineering, Virginia Tech, Blacksburg, VA 24061 USA (email: {acd1797, walids}@vt.edu).

W. Zuo is with the Department of Architectural Engineering, Penn State University, State College, PA 16801 USA (email: wangda.zuo@psu.edu).

R. Budiarto and D. Novitasari are with the Department of Nuclear Engineering and Engineering Physics, Universitas Gadjah Mada, Indonesia (email: rachmawan@ugm.ac.id, dwi.novitasari@mail.ugm.ac.id).

M. D. Koerniawan is with the Department of Architecture, Institut Teknologi Bandung, Indonesia (email: donny@ar.itb.ac.id).

We thank Yizhi Yang, John Zhai, Irawan Eko Prabowo, Lily Tambunan, Nissa Aulia Ardiani, Ferdi Mochtar, and Edward Syarif for the various discussions within the context of the Makassar project that helped scope some of the research.

introduces a variation of the traditional attention mechanism, called *ProbSparse* self-attention. The authors in [6] propose an encoder-only Transformer architecture, called the Time Series Transformer (TST), for performing both *multivariate* time-series regression and classification tasks. In [7], the authors develop a further extension of the forecasting Transformer architecture, called Spacetimeformer, which considers both the temporal and spatial relationships between sequence features for *multivariate* time-series regression. In contrast, the authors in [13] study the viability of attention mechanisms for the multivariate time-series forecasting task. Regarding computer vision, the authors of [8] propose the novel Vision Transformer (ViT) architecture with patch encoding scheme. The authors of [9] successfully apply Vision Transformer (ViT) architecture to the agriculture trade space, specifically distinguishing crops from weeds using aerial images. In [10], the authors also apply the ViT architecture to agriculture, identifying diseases of casava plants using images of their leaves. In contrast, the authors of [14] study the validity of vanilla ViT performance claims. Lastly, regarding data fusion, in [11], the authors apply Transformers to fuse images and LiDAR representations of space in autonomous driving tasks. Meanwhile, the authors of [12] propose a novel approach to multi-modal fusion learning, called Unified Transformer (UniT), which also doubles as a multi-task learning architecture.

However, approaches pertaining to time-series forecasting only focus on either univariate regression [3, 5], same-feature multivariate regression [6] (i.e., the features used as input are the same as those predicted at the output), or unique univariate target regression [4, 7, 13] (i.e., multiple input features and a single unique output feature). In terms of computer vision, while the results in [15] and [14] demonstrate the overall viability of ViT variations, and the authors of [9] and [10] prove that ViT can be applied to agriculture, they only focus on a limited set of images and classes, with the latter only examining diseases in cassava plants. Regarding data fusion, the limitations of [11] are two-fold: 1) the reliance on convolutional neural networks (CNNs) for feature extraction, rather than pure Transformer networks, and 2) the similarity between image and LiDAR data sources, both of which represent visual and spatial information. The former being less computationally efficient, and the latter lacking in feature diversity. Further, the work in [12] only focuses on image and text inputs, which are not representative of the environmental and temporal features present in S&CCs. Hence, there is a need for novel approaches which not only address these issues, but also consider their broader impact on the global community through application in S&CC environments.

## B. Contributions

The main contribution of this paper is the design of a novel Transformer-based AI framework for generalized IoT data fusion and multi-task learning in S&CCs. Our framework is built upon a backbone of purely Transformer encoder layers, and further customized through interchangeable input embedding and output task heads. This enables system deployments to learn from a variety of heterogeneous input data types from

IoT sources and output task types present S&CCs environments. Moreover, the extendable nature of the output heads facilitates learning multiple tasks parallel. We consider five unique problem sets for our framework, which were chosen to simulate the problem diversity in smart urban environments; these are 1) multivariate time-series forecasting of localized meteorological data, 2) plant health and disease classification using images, a fusion of both 3) multivariate time-series data and 4) images to perform individual forecasting and plant health classification tasks, and 5) a fusion of these same inputs to perform multi-task learning in parallel. Deployments of our framework are split across several input type (i.e., single-input, and multi-input) and task type (i.e., single-task, and multi-task) regimes. In the *single-input single-task* regime, a Transformer model is associated with each task and learns it using a single data source (i.e., time-series, images). In the *multi-input single-task* regime, a Transformer model is associated with each task, and learns it using a fusion of image and time-series data sources. Lastly, in the *multi-input multi-task* regime, a single Transformer model is used for all tasks, which it learns through input data fusion. All of our source code is publicly available on GitHub<sup>1</sup>.

We run extensive experiments to evaluate the performance of our framework. The results show that the proposed Transformer-based system can indeed handle various input data types via custom sequence embedding techniques. Our results also demonstrate that the Transformer system is well-suited to learning heterogeneous task sets. We also compare our Transformer-based models against competitive non-Transformer variants for each task. Specifically, our comparisons show that our proposed framework either maintains or exceeds the performance capabilities of non-Transformer baselines. In addition, we observe that multi-task learners exhibit both increased memory and computational efficiency while also maintaining comparable performance to both single-task variants and baselines. This affinity demonstrates the flexibility of Transformer networks to learn from a fusion of IoT data sources, their applicability in S&CC trade spaces, and their further potential for deployment on edge computing devices.

The rest of this paper is organized as follows. Section II presents the system model. In Section III, we propose Transformer architectures for multi-variate time-series regression, visual plant disease classification, single-task data fusion, and heterogeneous multi-task learning tasks. Section IV provides simulation results. Finally, conclusions are drawn in Section V.

## II. SYSTEM MODEL

We consider the design and deployment of an AI framework within S&CC environments in which there are networks of IoT sensors. These sensors collect a wealth of visual, spatial, and ecological data from within the city. This information paints a picture of how the city is jointly effected by these factors, and their relationship can then be used to bolster positive growth and development.

<sup>1</sup><https://github.com/news-vt/makassar-ml>

A real-world example of this kind of environment is Makassar City, Indonesia. Makassar is the 5<sup>th</sup> largest urban center in Indonesia, with a population of 1.7 million [16], and aims to become a world-class metropolis through combining both IoT and AI to transform many of its 7,520 alleyways into smart and sustainable gardens. Supported by the U.S. National Science Foundation (NSF) and the U.S. Department of State, the Smart Garden Alley Project<sup>2</sup> proposes to develop *smart* garden alleys following a biomimetic philosophy; this represents the garden alleys, IoT sensor networks, and AI-informed government policy as a collection of cells, nerves, and a brain.

We formulate the design of an AI framework for S&CC environments, like Makassar City, as problems of both *data fusion* and *multi-task learning*. The variety of data available to IoT sensor networks necessitates the design of AI that can both input diverse feature types, such as visual and ecological, while also learning relationships between them. Likewise, the variety of tasks that can be performed using the IoT data, such as classification and forecasting, further necessitates AI that can not only implement these heterogeneous tasks, but also learn the relationships between them.

#### A. Heterogeneous Data Fusion

We now formulate the problem of heterogeneous data fusion in S&CC environments. Next-generation AI systems for S&CC must learn to leverage a fusion of IoT data sources to perform necessary tasks. This facilitates learning relationships between loosely-correlated environmental characteristics, and encourages generalization through diverse fusion of these features. However, the design of such AI systems which use these diverse feature sets is non-trivial. In particular, special considerations must be made for both data preprocessing and the overall AI architecture.

With regards to preprocessing, the frequency of each input feature set matters significantly for ingestion into the model. Consider for example time-delimited meteorological data as one feature set, which may have an hourly frequency. If the task necessitates fusion with images, the question arises of how to combine static image frames with this time-delimited data. The key point here is that, while many algorithmic approaches to this fusion are viable, special consideration must be made to formulate a preprocessing algorithm in general. This in turn adds increased layers of complexity to the overall system design.

With regards to the overall AI architecture, several considerations must be taken into account when fusing diverse feature sets. Extrapolating from the aforementioned data frequency concern, this also affects the design of model input layers as well as any embedding schemes. In particular, traditional AI design assumes inputs to be supplied in discrete increments, and the frequency the data affects the overall input shape. Consider the previous example in which time-delimited data is fused with images. If static images are supplied, then an input layer must be designed to accept just a single image. However, if the preprocessing algorithm instead produces multiple

images in a buffer, then the design of the input layer must change to support a sequence of frames. Likewise, knowledge of the input shape will affect the downstream embedding schemes, which could completely change the AI architecture. For example, single-image embedding could pool the matrix pixels, whereas multi-image embedding could instead project the sequence of frames. The key point is that the fusion of diverse feature sets is non-trivial, and affects the entire AI architecture design.

#### B. Multi-Task Learning using Attention

Now, we formulate the problem of multi-task learning of diverse task sets in S&CC environments using attention-based Transformer architectures. Highly-performant AI language models such as BERT [17], XLNet [18], and GPT-3 [19] all use attention mechanisms and Transformers as their baseline architecture. The dominance of Transformers has extended beyond fields of NLP, finding applications in computer vision with models such as the ViT [8], and time-series forecasting with models such as the Temporal Fusion Transformer (TFT) [3] and Informer [4]. However, all of these models are designed with a *singular input data type* in mind (i.e., text, images, time-series, etc.). In the presence of multiple data types, none of the aforementioned architectures alone can learn correlations between the heterogeneous feature sets. Consider now our system model of IoT sensor networks in urban environments, as shown in Fig. 1. There exists many sensory features from these devices, such as meteorological information, traffic camera video feeds, and citizen mobility from wireless networks that can be leveraged to bolster smart city growth and development. In addition to diverse feature sets, each data collection is often also associated with more than one task. Consider for example the fusion of time-series meteorological data and images of plants as discussed in Section II-A. Using both inputs, it is possible to perform multiple tasks such as forecasting meteorological events, predicting necessary irrigation changes to promote plant growth, and even identifying the onset of disease. Next-generation AI systems for deployment in S&CC environments must be able to leverage diverse feature sets such as these to make more tailored decisions. As such, one key goal of this paper is to design and implement an AI framework which learns to S&CC growth using a fusion of heterogeneous features.

In light of the Transformer's affinity across diverse trade spaces, we propose to exploit them in the context of smart cities, because they are capable of learning heterogeneous feature correlations for a variety of tasks in parallel fashion. The Transformer assumes inputs to be of an embedded sequential nature, but is agnostic to task-specific nuances. This generalizability makes the Transformer architecture a prime choice for implementing fusion models, as many data types can be represented using sequence-based embedding schemes. Hereinafter, we refer to the process of learning relationships between these diverse feature sets as *data fusion*, and the art of learning multiple tasks as *multi-task learning*. Data fusion correlates features from multiple input sources via timestamp or geographic location and fuses them within the Transformer

<sup>2</sup><https://sites.psu.edu/sbslab/research/city/smart-garden-alleys/>

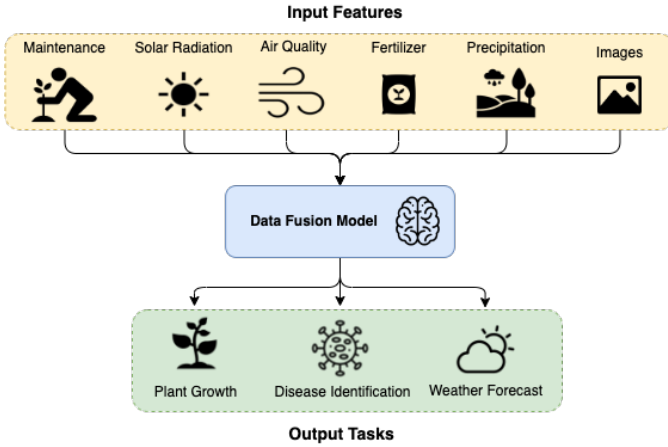


Fig. 1. An example of Data Fusion Learning in smart city environments. Input features such as city maintenance, solar radiation, air quality, fertilizer, precipitation, and images can be fused to learn plant growth, disease identification, and meteorological forecasting tasks.

network. Multi-task learning extends this relation of input features to learning several tasks across various trade spaces in parallel. During training the network optimizes losses for each output task concurrently, allowing a single model to learn from shared experience and thereby boosting generalization performance. Several challenges arise in the process of designing Transformer architectures tailored for data fusion and multi-task learning. Feature diversity in both dimension and physical properties are challenges in data fusion. For example, image and meteorological datasets have completely unique shapes (e.g., pixels with RGB color channels, multivariate time-series, etc.) and value units (e.g., pixels in range 0-255, hourly temperature in Celsius, etc.). The challenge is designing a fusion technique which takes these properties into account and learns across appropriate sequence dimensions. Likewise, task diversity is a challenge in multi-task learning. The challenge is designing an AI architecture such that its core framework supports the diverse dimensionality requirements of the output tasks (e.g., RGB image generation, 24-hour meteorological forecast, etc.) and capability for various multivariate projections (e.g., sinusoidal, exponential, etc.). Next-generation AI systems for S&CC deployments can greatly benefit from both data fusion and multi-task architecture design choices to leverage the wide array of IoT sensor data available.

In the following section, we address the aforementioned challenges and propose Transformer architectures for data fusion and multi-task learning.

### III. TRANSFORMER NETWORKS FOR SMART CITIES

We propose five Transformer-based architectures that are tailored specifically to smart city task sets. In particular, we focus on five specific supervised-learning problems which simulate the tasks encountered in S&CCs, like Makassar City. These tasks are divided into two different categories for *single-task* and *multi-task* learning.

In the single-task category, we first formulate a supervised multivariate time-series regression task. Specifically, unique input features within a historical time window are used to

predict a separate set of features along a finite-time horizon. Second, we formulate a plant health identification task using images labeled with various healthiness categories (i.e., healthy, diseased, etc.). In this task, a single image is used as input to predict a class label. Third, we formulate a variation of the regression task that fuses both time-series and image datasets to enhance performance. In this task, a model accepts both a single image and a window of multivariate time-series data as input. The model then uses this information to predict a unique set of output features along a finite-time horizon, similar to the single-input case. Fourth, we formulate a plant health classification task using a fusion of the aforementioned datasets. Here the same image and time-series window are used as input, whereas now the model predicts the probability distribution over a finite set of class labels.

In the multi-task category, we extend the single-task data fusion problems to perform both heterogeneous tasks simultaneously using a single model. Specifically, we fuse both static images and multivariate time-series windows as input, and use this information to predict both the healthiness class label and a set of output features along a finite-time horizon. This configuration allows a single AI model to optimize multiple tasks in parallel, while also benefiting from shared experience.

#### A. Forecast Transformer for Multivariate Regression

We propose the Forecast Transformer (FoT) architecture for supervised time-series regression of multi-input and multi-output feature spaces. This model was developed in conjunction with an application to the financial trade space in mind. Specifically, forecasting stock market asset valuations using multiple unique feature sets. Naturally, this can be directly applied to our smart city problem, as many tasks involve the computation of arbitrary output values as a function of some input. In the case of urban farming, the input could, for example, be multivariate time-series meteorological data, which is then used to predict output features such as plant irrigation requirements and expected crop yield. A key point of the FoT design is that it is agnostic to any specific regression task. Specifically, a clear advantage of this architecture over alternative competitive models is its portability to multiple trade spaces, given generalized time embedding schemes, and its ability to learn arbitrary multivariate sequence relations.

At its core, the FoT architecture uses a pure-encoder approach to time-series regression. Time-series relations are learned through encoding a multivariate input sequence through cascaded `TransformerEncoder` layers. These layers employ multi-head self-attention mechanisms [2] to learn both cross-feature and cross-sequence-index relations within the given input sequence. This is in contrast to the traditional NLP Transformer design, which uses both encoder and decoder layers for sequence-to-sequence translation. In addition, the model employs a Time2Vec (T2V) [20] embedding layer, which learns a vector representation of the input time sequence. The architecture is made dynamic via hyperparameters which control the length of the input sequence, number of input features, number of output features, number of fully-connected sub-layers, embedding dimension, number

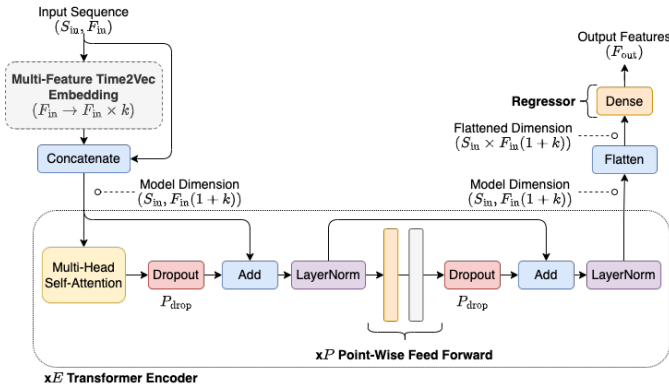


Fig. 2. FoT model architecture. Blocks without names are Dense (orange), GeLU activation (gray), Linear activation (green), and Dropout (red).

of cascaded encoder layers, encoder point-wise feed forward dimension, and number of self-attention heads per encoder. The design of the FoT architecture is shown in Fig. 2.

1) *Multivariate Time2Vec Embedding*: Historically, RNNs have been the tool of choice for sequence-based modeling and regression. The auto-regressive nature of the general RNN design allows it to learn inter-element relations using an element’s *index*, or more generally *location*, within a given input sequence. In the case of Transformers, entire sequences are processed at once in Attention layers via matrix dot products. This means that the sequence information gathered via auto-regression in RNNs is lost in the presence of Attention-based networks. To overcome this issue for NLP-related tasks, the original Transformer architecture adopted a fixed position-encoded embedding scheme, which represents an element’s position within a sequence as a sinusoid of varying frequencies [2]. In working with time-series data, however, this encoding scheme fails to capture the time information of an element relative to the overall dataset (i.e., hourly, daily, or monthly frequencies). We overcame this issue by implementing a variation of the T2V embedding scheme proposed in [20], which we call *multivariate Time2Vec (MT2V) embedding*. This embedding scheme performs two tasks within the network. First, it acts as an embedding layer that represents the input features as vectors in higher-dimensional space. Second, it captures the real time periodicity of each input feature by learning both linear and periodic components and using these as the vector embedding; akin to a learned Fourier Series representation. Mathematically, our MT2V embedding scheme extends the definition of [20] to multivariate input vectors, instead of simple scalar inputs. Given an input feature vector  $\tau$  with  $F_{in}$  feature dimensions, and a total embedding dimension  $k$ , the embedding scheme MT2V of  $\tau$ , denoted as  $MT2V(\tau)$ , is a 2-dimensional matrix defined as

$$MT2V_{ij}(\tau) = \begin{cases} \omega_{ij}\tau_i + \phi_{ij}, & \text{if } j = 0, \\ \mathcal{F}(\omega_{ij}\tau_i + \phi_{ij}), & \text{if } 1 \leq j < k, \end{cases} \quad (1)$$

where  $\omega$  is a learned frequency matrix with shape  $(F_{in}, k)$ ,  $\phi$  is a learned phase shift matrix with shape  $(F_{in}, k)$ ,  $\mathcal{F}$  is a periodic function (i.e.,  $\sin$ ,  $\cos$ , etc.), and  $MT2V_{ij}(\tau)$  is the  $i$ ’th feature and  $j$ ’th embedding dimension of the learned

embedding matrix with shape  $(F_{in}, k)$  for the given input feature vector. In practice, the feature and embedding dimensions are flattened to create a single vector with  $F_{in} \times k$  dimensions. This allows the embedding to be repeated along the sequence dimension  $S_{in}$  to create a final sequence embedding matrix with shape  $(S_{in}, F_{in} \times k)$ , which is more easily ingested into the Transformer attention layers. The final step of the embedding process, prior to feeding into the Transformer encoder layers, is to concatenate the original batched sequence input with shape  $(B, S_{in}, F_{in})$  with the MT2V embedding output, resulting in a final encoder input with shape  $(B, S_{in}, D_e)$ , where  $D_e = F_{in}(1 + k)$  is the inner model dimension of the Transformer encoder.

2) *Transformer Encoder Layers*: The core of the network is the Transformer Encoder, which is comprised of cascaded TransformerEncoder layers. The design of these layers is similar to those proposed in [20], with some minor changes to be compatible with time-series data. Each layer consists of a two concise sub-layers. The input to the encoder layer is a matrix with shape  $(B, S_{in}, D_e)$ , where  $B$  is number of batches,  $S_{in}$  is the input sequence length, and  $D_e$  is the inner model dimension (derived from the MT2V embedding output shape). In the first sub-layer, the encoder input passes through a multi-head self-attention layer [20], which learns, or “attends” to, cross-element and cross-feature importance of the input. The output of this attention layer (also a matrix of with shape  $(B, S_{in}, D_e)$ ) passes through a dropout regularization layer with probability  $P_{drop}$ , and then gets added to the original encoder input to form a residual and normalized using a LayerNormalization layer. The output of this normalization passes through the second sub-layer, which consists of a point-wise feed forward network (called PointWiseFeedForward), followed by another sequence of dropout, residual addition, and layer normalization. The point-wise feed forward network acts as a cascaded series of convolutions with a kernel size of 1, which upscales and then downscales the attention output into separate feature dimension  $D_{ff}$  respectively. The number of encoders  $E$ , number of self-attention heads  $h$ , embedding factor  $k$ , feed-forward dimension  $D_{ff}$ , and dropout regularization rate  $P_{drop}$  are controlled via hyperparameters.

3) *Fully-Connected Regressor*: Up to this point in the network, the model has learned a time vector embedding and cross-feature relations through attention mechanisms in the encoder layers. To actually perform multivariate regression, the encoder output (recall having shape  $(B, S_{in}, D)$ ) must be mapped to the desired output sequence length and number of output features. In this paper we only consider output sequences with length 1 (i.e., 1 day in the future) to simplify the architecture design. However, it should be noted that the design could be extended to support longer sequences in future works. The output feature mapping can therefore be achieved using a single fully-connected layer with *linear* activation as the final layer of the model. This final regressor layer maps the result of the previous fully-connected layers to the desired output feature space (akin to a classification layer in classifier networks, sans softmax activation).

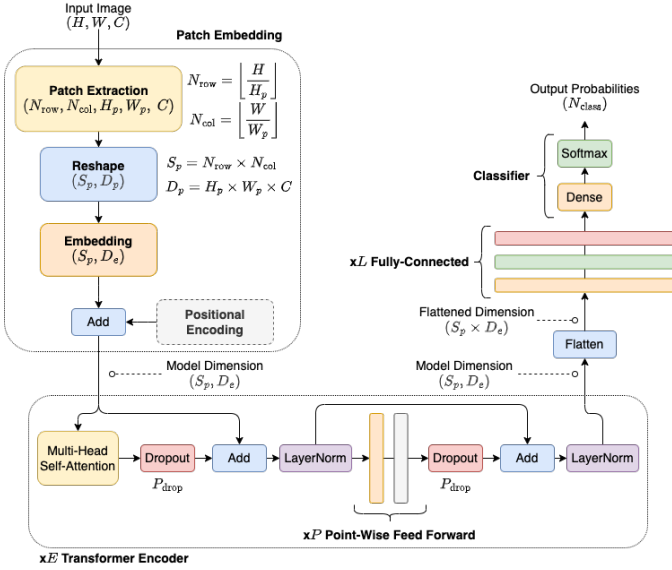


Fig. 3. ViT model architecture. Blocks without names are Dense (orange), GeLU activation (gray), Linear activation (green), and Dropout (red).

### B. Vision Transformer for Plant Health Identification

We propose a variation of the well-known ViT [8] architecture for computer vision tasks in smart city environments. This facilitates learning image features using attention mechanisms, which maintains a similar architecture structure to that of the aforementioned time-series regression task, and also has been known to exceed performance over competitive CNN models.

Similar to the FoT, the ViT also leverages the same underlying pure-encoder Transformer architecture for learning image feature correlations. The primary difference between them is in the underlying embedding scheme. Images are single static objects, but the Transformer attention mechanism requires sequence-based input to learn relationships. To make an image compatible as input, the ViT applies a patch extraction algorithm which converts a static image into a sequence of small square subset frames akin to a checkerboard. These patches are then projected (embedded) into a higher dimensional space matching the input dimension of the cascaded `TransformerEncoder` layers. The output of the encoders is then passed through a cascaded sequence of fully-connected layers, and subsequently a final dense classification layer for classification tasks. The ViT architecture is made dynamic via multiple hyperparameters which control the number of patches, patch shape, number of fully-connected sub-layers, embedding dimension, number of cascaded encoder layers, encoder point-wise feed forward dimension, and the number of self-attention heads per encoder. The design of the ViT architecture is shown in Fig. 3.

1) *Image Patch Generation*: Historically, CNNs have been used as the standard for image-based machine learning (ML) tasks. Convolution-based networks were originally proposed by Lecun *et al.* [21] for document character recognition in 1998, and then popularized in 2012 by Krizhevsky *et al.* [22] for successful application to object classification tasks. CNN architectures take as input source images with 3 dimensions of

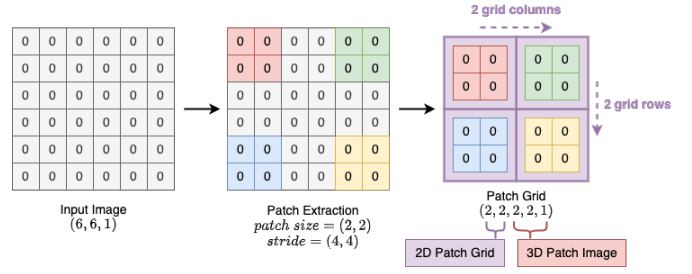


Fig. 4. Example of patch extraction algorithm. An input image (left: gray) with shape (6, 6, 1) pixels is split into 4 patches (middle: red, green, blue, yellow) using patch shape of (2, 2) and stride of (4, 4). The patches are coalesced into a grid (right) of shape (2, 2, 2, 2, 1).

( $W, H, C$ ), where the former two refer to the image width and height, and the latter the number of color channels (i.e.,  $C = 1$  for grey-scale,  $C = 3$  for RGB, etc.). Convolutional layers within a CNN learn to extract features from source images by performing matrix dot-product operations on small windowed regions commonly referred to as a *kernels*. These kernels are convolved with the input image using various settings for padding and stride offsets which filter the pixels within the region down to a single value. Multiple kernels can be applied in parallel to project the resulting convolved image into higher or lower channel dimensions, thereby varying the number of features that can be extracted from a single image.

In contrast, the ViT architecture learns image features by first splitting a source input image into multiple smaller regions called *patches*. The algorithm generates patches similar to a convolution. Patches are extracted using a kernel with shape ( $H_p, W_p$ ) which copies source pixels within its region. This kernel is then convolved with the input image using a stride offset to pad the distance between each region from its nearest neighbors. The patch extraction operation results in a output matrix with shape ( $N_{row}, N_{col}, H_p, W_p, C$ ), where ( $N_{row}, N_{col}$ ) are the number of rows and columns in the resulting patch grid, ( $H_p, W_p$ ) are the width and height of each patch, and  $C$  is the number of channels in the original input image. In practice, the patch matrix for a single image is flattened into shape ( $S_p, D_p$ ), where  $S_p = N_{row} \times N_{col}$  serves as the sequence dimension for the Transformer encoder, and  $D_p = H_p \times W_p \times C$  serves as the patch projection dimension. Knowing the original patch size and number of color channels allows the user to extract the resulting patches individually for closer inspection.

To better understand the patching algorithm a simple example is shown in Fig. 4. In this example, an arbitrary input image with shape (6, 6, 1) is passed to the extraction algorithm using a patch shape of (2, 2) and stride of (4, 4). The image is split into 4 unique patches which are organized into a matrix with shape (2, 2, 2, 2, 1), where the first 2 dimensions are the patch grid (2, 2), and the latter 3 are the patch image (2, 2, 1).

Further, a demonstration of the patch extraction algorithm on a real image is shown in Fig. 5. Here, an RGB image with shape (256, 256, 3) is used as input. Using a patch size of (18, 18), and a stride offset of (18, 18), the image is split into

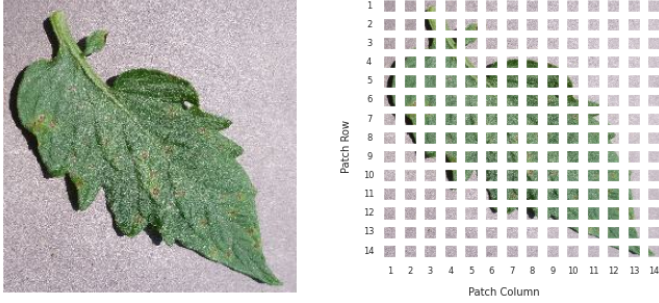


Fig. 5. Demonstration of patch extraction algorithm result. Input image (left) with shape  $256 \times 256$  pixels is split into 196 patches (right,  $14 \times 14$  grid) each with shape  $18 \times 18$  pixels.

196 unique patches along a  $14 \times 14$  grid<sup>3</sup>. Notice that, since the patch size and stride offset are the same, the resulting patches will completely cover the original image with no omitted pixels.

To incorporate the patch extraction algorithm into the ViT architecture, we designed a static TensorFlow layer called `Patches`. The advantage of this approach is that the layer can be directly inserted into model build or even preprocessing pipelines to dynamically extract patches from batches of input images. The layer is made dynamic through hyperparameters such as patch size and stride offset which tune the resulting patch dimensions. Note that, by default, the patch size and stride offset are the same so as to have complete coverage of the input image.

2) *Image Patch Embedding*: Before image patches can be fed into the `TransformerEncoder` layers they must first be projected into the same inner dimension of the encoder. Recall that output of the patch extraction algorithm for a single image is a matrix of shape  $(S_p, D_p)$ . However, the Transformer encoder requires the input to have dimension  $(S_p, D_e)$ , where  $D_e$  is the encoder inner dimension. Therefore, an embedding scheme must be applied which projects the patch dimension  $D_p$  to the encoder dimension  $D_e$ . In addition, the embedding must also incorporate the sequential information of the patches as the Transformer attention mechanism processes all sequence input concurrently. To accomplish this, we built a custom `PatchEncoder` layer which does both tasks. First, a fully-connected layer is used to learn the projection  $D_p \rightarrow D_e$ . Second, a relative positional embedding is added to the projection to encode the sequence information for each patch. The result is a matrix of shape  $(S_p, D_e)$  which can be fed directly into the Transformer encoder layers.

### C. Fusion Transformer for Multi-Task Learning

Up to this point, our proposed model designs used each input data set independently to perform a single task. In particular, FoT only uses multivariate sequential data for regression, and ViT only uses images for classification. This compartmentalization of data and tasks results in several AI models being required for a single system. Depending on the environment,

<sup>3</sup>The number patches along each row or column is computed as  $N_{\text{row}} = \lfloor \frac{H}{H_p} \rfloor$  and  $N_{\text{col}} = \lfloor \frac{W}{W_p} \rfloor$  respectively

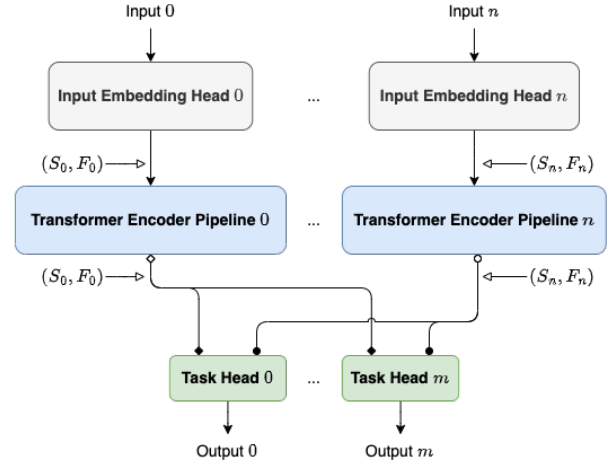


Fig. 6. High-level outline of the FuT model architecture for data fusion learning. Each input source has its own embedding head (gray) and Transformer encoder pipeline (blue). The outputs of each encoder pipeline are then passed through task-specific output head (green). The number of embedding head and encoder pipeline pairs  $n$  is dependent on the amount of input desired, and the number of task heads  $m$  is dependent on the application.

this separation may be required. In IoT environments, however, where the data is loosely-correlated (i.e., weather and time-stamped images), it would be more efficient for a single model to input a fusion of heterogeneous input data sets and learn to perform multiple tasks in parallel. Hence, we propose the Fusion Transformer (FuT), which combines the techniques of the aforementioned FoT and ViT architectures for both single-task data fusion and multi-task learning. Data fusion is critical in IoT applications where data collection sources are plentiful, and the data itself is often time-correlated. Examples of such data in smart city environments include weather data from meteorological sensors, and images from video cameras placed on street corners. Using the example of Makassar City’s smart garden alleys, the FuT architecture facilitates building an AI nerve-center for the city that can leverage a fusion of the various IoT data sources at its disposal to forecast plant health and environmental conditions.

The core of the FuT model is a Y-network where each branch acts as an encoding pipeline that is uniquely associated with each input data source. The output of these pipelines are fed into task-dependent output blocks, referred to as *task heads*, that fuse the learned encodings for all input data sources and applies them to learn a specific task (i.e., classification, regression, etc.). A high-level view of the FuT architecture is shown in Fig. 6. Note that the number of input embedding heads and Transformer encoder pipelines  $n$  are tightly coupled, meaning that each input head is directly linked to a specific pipeline. In contrast, the number of task heads  $m$  is independent of the input pipelines, and can therefore be chosen relative to the desired tasks.

The interchangeable nature of the task head was specifically designed with transfer learning applications in mind. Transfer learning is a process by which a sub-section of a pre-trained model is grafted into a new architecture for a potentially different application [23]. This means that the new overall

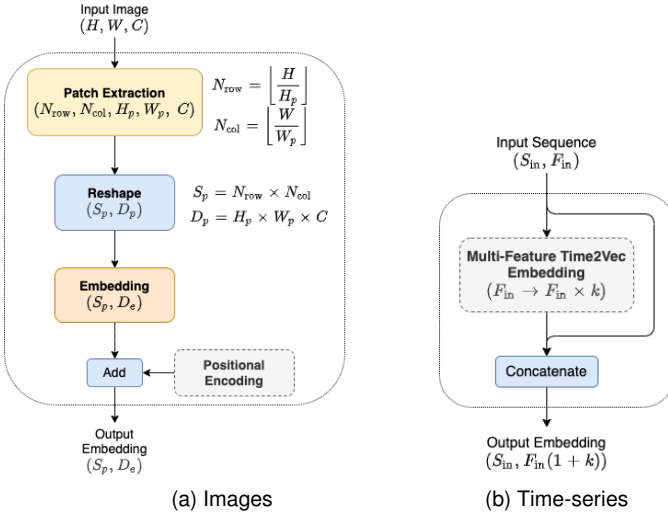


Fig. 7. Examples of FuT input embedding heads for (a) images and (b) multivariate time-series datasets.

model can benefit from the experience that the pre-trained stub has learned. In FuT, the encoder pipelines for each input branch can be pre-trained and grafted into a new output head to learn a different task. Further, FuT supports multi-task learning frameworks with the option for multiple output task heads. This emphasis on both transfer learning and multi-task learning offers many benefits to S&CCs as its needs and requirements change over time. For example, initial models could fuse time-series meteorological data and images of plants to forecast irrigation requirements. If the city then desires to add the capability of identifying plant diseases, a classification head can be appended to the pre-trained base model to accomplish both tasks simultaneously.

1) *Input Embedding Heads*: Each branch of the Y-network is dedicated to encoding a specific input data source using cascaded `TransformerEncoder` layers. The input to each pipeline is a pre-embedded 2-dimensional input sequence. This generalization decouples the input data embedding scheme from the model, thereby making it agnostic to any specific input data sources. It is therefore the job of data-specific input heads to perform embedding and reshaping operations which ultimately conform to the encoding pipeline format. Gleaning from techniques used in ViT and FoT Transformers, we extract the embedding sections of these networks and encapsulate them as self-contained embedding layers for image and multivariate time-series data respectively. Examples of these embedding heads are shown in Fig. 7.

The image embedding head in Fig. 7a accepts 3-dimensional images of shape  $(H, W, C)$  and extracts patches according to the algorithm discussed in Section III-B1. These patches are then reshaped into a 2-dimensional matrix and embedded according to the technique described in Section III-B2. Note that here we also add a positional encoding to capture the sequential nature of the image patches in the attention mechanism. This produces a 2-dimensional matrix of shape  $(S_p, D_e)$ , where  $S_p$  is the number patches and  $D_e$  is the patch embedding dimension. The newly-encoded patches are then passed directly to an associated Transformer encoder pipeline

to learn feature relations.

The time-series embedding head in Fig. 7b accepts 2-dimensional multivariate sequence data of shape  $(S_{in}, F_{in})$ , where  $S_{in}$  is the sequence length and  $F_{in}$  is the number of input features. These features pass through a MT2V embedding layer, as discussed in Section III-A1, which represents the time-series information as a Fourier series. This Fourier series representation is then combined with the original input via a concatenation layer along the feature dimension to form a 2-dimensional matrix of shape  $(S_{in}, F_{in}(1+k))$ , where  $k$  is the MT2V embedding factor. Similar to the image embedding head, the output of the time-series embedding head is also passed directly to an associated Transformer encoder pipeline to learn feature relations.

A particular point about these input heads is the shape of its associated output. Each produces a 2-dimensional output matrix with shape  $(S, F)$ , where  $S$  is the sequence length and  $F$  is the number of embedding features. Notice that the sequence length and feature size are tightly coupled with the input data. This standardization to a 2-dimensional form ensures that all embedding outputs are compatible with Transformer encoder pipelines, which assume 2-dimensional input matrices.

2) *Data Encoding Pipelines*: After the input data passes through each respective embedding head it is fed through a cascaded sequence of `TransformerEncoder` layers that are unique to the branch. The operation of these layers is similar to those discussed in Section III-A2. It is important to note that Transformer encoders maintain the dimensionality of their input data; meaning that the shapes of both input and output matrices are identical. In FuT, each branch maintains the original shape of its embedding head. This is important because, depending on the embedding scheme, the resulting length and number of features for each sequence could be different. This approach was chosen, however, to make the encoders for each branch unique to the sequences they learn. It is then the job of the following task-specific output head to choose how the sequences are fused.

3) *Task-Specific Output Heads*: After the input data passes through its respective Transformer encoder pipelines, the output of each pipeline is then fused together at the final block of the network, referred to as a *task head*. The task head is interchangeable based on the desired ML task, and multiple heads can be combined in parallel to build a multi-task learning framework. This interchangeable nature of input heads and output heads provides sufficient generalizability to learn the variety of tasks present in smart city environments.

As input, the task head has access to all encoder pipeline outputs at its disposal. The core Y-network learns encoded forms of the original input, and the self-contained task head learns how to fuse these encodings to learn a specific task. Separating the pipelines like this gives the task head full control over how the learned encodings are fused together, which further generalizes the architecture design.

In Fig. 8, we give examples of designs for both classification and regression task heads. Note the similarities between ViT and FoT architectures, as discussed in Sections III-A and III-B respectively. The final task-specific layers of these models have been encapsulated within interchangeable blocks. This allows

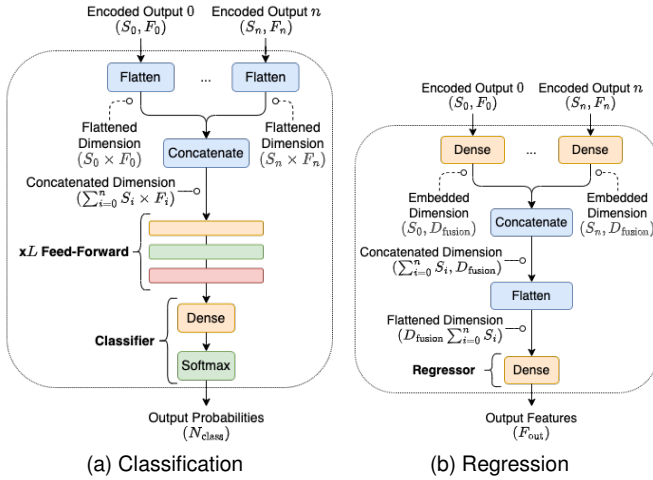


Fig. 8. Examples of FuT output heads for (a) classification and (b) regression tasks. Blocks without names are Dense (orange), ReLU activation (green), and Dropout (red).

encoded forms of both input data types to be fused to enhance performance for each task.

The classification head in Fig. 8a takes the outputs from  $n$  encoder pipelines with shapes  $(S_0, F_0), \dots, (S_n, F_n)$ , flattens them down to 1-dimensional vectors, and concatenates them resulting in a single vector with shape  $(S_0 \times F_0 + \dots + S_n \times F_n)$ . This vector is then passed through a fully-connected network with ReLU activation and dropout regularization. The final step is a dense classification layer with softmax activation to compute probabilities for each class.

The regression head in Fig. 8b also takes the outputs from the  $n$  encoder pipelines with shapes  $(S_0, F_0), \dots, (S_n, F_n)$  and projects each independently into a common feature dimension  $D_{\text{fusion}}$ . This results in  $n$  sequences with shapes  $(S_0, D_{\text{fusion}}), \dots, (S_n, D_{\text{fusion}})$ . This projection is critical as it allows the encoder outputs to be combined along the sequence dimension to form a unified encoded matrix with shape  $((S_0 + \dots + S_n), D_{\text{fusion}})$ . This matrix is flattened and then passed through a fully-connected regression layer with linear activation to compute the output features with dimension  $F_{\text{out}}$ .

There are two important points about these two example task heads. First, notice that both use the data from all encoder pipelines in different ways. Specifically, the classification task head in Fig. 8a flattens each pipeline matrix prior to concatenation, whereas the regression head in Fig. 8b first projects the features of each pipeline matrix to a common dimension and then concatenates these projections along the sequence dimension to form a single unified sequence. The second point is that the outputs of each head are unique and independent of the others, which is subtle yet critical. This means that the model can learn heterogeneous tasks simultaneously using the same input data. In addition, this design also provides the flexibility for the AI system to grow in conjunction with the smart city. This means that as the needs of the city evolve over time, so can the AI system with the capability for interchangeable output heads. If new tasks are required in the future, custom task heads can be created to generate the necessary output.

## IV. SIMULATION RESULTS

For our simulations, we examine the performance of the FoT, ViT, and FuT architectures presented in Sections III-A to III-C respectively. In Section IV-A, we detail a multivariate time-series regression task to demonstrate the performance of the FoT model in comparison with a non-Transformer baseline. In Section IV-B, we detail a plant disease identification task to demonstrate the performance of the ViT model, and also define a non-Transformer baseline for comparison. In Section IV-C, we detail two fusion learning experiments, combining images and time-series data for regression and classification tasks, and demonstrate the performance of the FuT model with a *single* output head (i.e. single-task mode). In Section IV-D, we detail an experiment for multi-task learning using the fusion of images and time-series data to demonstrate the performance of the FuT model with *multiple* output heads (i.e., multi-task mode). Finally, in Section IV-E, we compare model performance across all tasks. All models were trained for 30 epochs and a batch size of 256 on Virginia Tech’s Advanced Research Computing (ARC) high-performance computing (HPC) cluster.

### A. Multivariate Time-Series Forecasting

In this task, we consider the Beijing PM2.5 [24] dataset, with a history window of 24 hours to predict a horizon of 1 hour. These windows were selected due to their small size (i.e., easier to train) and relative periodicity (i.e., consider what occurred in the past day to predict 1 hour into the future). Specifically, we train the FoT model to take an input sequence of  $S_{\text{in}} = 24$  consecutive hours with  $F_{\text{in}} = \{\text{TEMP}, \text{DEWP}, \text{PRES}, \text{Iws}\}$  input features per hour, which are *temperature*, *dew point*, *pressure*, and *wind speed* respectively. The FoT model then predicts a horizon of  $S_{\text{out}} = 1$  hour with  $F_{\text{out}} = \{\text{pm2.5}, \text{Ir}\}$  output features, which are *air quality*, and *inches of rain* respectively.

To fully examine the performance of our proposed FoT architecture, we also evaluated a non-Transformer variant as a baseline for comparison. In the case of unique multivariate regression, we considered an LSTM architecture, which has historically been a top-performer in many regression trade spaces. In terms of parameters, for the LSTM model we chose 3 cascaded LSTM layers with 1024, 512, and 256 units each, followed by 2 fully-connected layers with 128, and 64 units each, and 10% dropout regularization. Note that here we only train a single baseline LSTM model, instead of hyperparameter tuning. This decision was made intentionally to reduce experiment complexity, directing resources to focus on tuning the proposed models rather than the baselines. We therefore selected this static set of LSTM network parameters using intuition from previous experience in the financial trade space.

The data was distributed using a train/val/test percentage split of 70/20/10 respectively. This subset size was chosen such that our models would have sufficient historical data to learn periodic trends between seasons. The FoT models were optimized using the Adam optimizer coupled with various learning rate schedules as tuneable parameters to stabilize

performance. We minimize mean squared error (MSE) loss and use mean absolute error (MAE) as an added metric to indicate performance.

### B. Plant Disease Classification

In this task, we consider images in the Plant Village [25] dataset to predict a probability distribution across 38 healthiness class labels. All images are resized to shape  $(72, 72, 3)$ , and scaled to range  $[0, 1]$ . In addition, the training and validation images are augmented with random flips in both the vertical and horizontal axes.

To fully examine the performance of the ViT architecture, we also evaluated a non-Transformer variant for comparison on the plant disease identification task. Here, we considered the well-known InceptionV3 [26] architecture, which is based on CNNs. A ready-to-use implementation of this architecture is provided through the TensorFlow API<sup>4</sup>, which we employed to simplify experiment complexity. However, note that for this experiment we trained an InceptionV3 model from scratch; that is, we did not use any pre-trained weight options. This is an important distinction, as TensorFlow provides the option for InceptionV3 variants which have been pre-trained on the ImageNet [27] dataset. In addition, as the InceptionV3 model was provided through TensorFlow, its design is more rigidly defined compared to custom implementations. This prohibits most of the hyperparameter tuning options that we employ with our custom models. Therefore, because of this, we only trained a single InceptionV3 model using the built-in parameter list.

The data was distributed using a train/val/test percentage split of 70/20/10 respectively. The ViT models were optimized using the Adam optimizer coupled with a constant learning rate of  $10^{-4}$ . We chose a constant learning rate here as our preliminary tests indicated that the ViT model was less sensitive to changes in learning rate, and therefore did not require a decay schedule in contrast to the regression tasks. We minimize the sparse categorical crossentropy (SCCE) loss, and we use accuracy as an added metric to indicate performance.

### C. Data Fusion Learning

In this task, we consider a fusion of the Plant Village and Beijing PM2.5 datasets to ensure fair performance comparison between FoT and ViT models. Just like in the classification task, all images are resized to shape  $(72, 72, 3)$ , rescaled to range  $[0, 1]$ , and augmented to improve generalization. Likewise for the time-series dataset, we consider an input sequence of  $S_{in} = 24$  consecutive hours with  $F_{in} = \{\text{TEMP}, \text{DEWP}, \text{PRES}, \text{Iws}\}$  input features per hour to predict a horizon of  $S_{out} = 1$  hour with  $F_{out} = \{\text{pm2.5}, \text{Ir}\}$  output features.

### D. Multi-Task Learning

In this task we again consider a fusion of the Plant Village and Beijing PM2.5 datasets to ensure fair performance comparison with FoT, ViT, and FuT models with single output

heads. All input data pre-processing for this experiment is equivalent to the single-head fusion experiments discussed in Section IV-C.

Because the multi-task FuT architecture has multiple output heads, each head is given its own loss and metrics to optimize. The regression head uses MSE loss with MAE metric, and the classification head uses SCCE loss with accuracy metric. These losses are aggregated using weighted mean into a single loss value for each train/val/test category to optimize the overall model. Model performance can therefore be examined either for each individual head (using its associated loss), or for the entire model using the aggregated loss.

### E. Performance Comparison

For each of the tasks discussed in Sections IV-A to IV-D we train 48 hyperparameter variations of our FoT, ViT, single-task FuT, and multi-task FuT models. The best configuration for each model is identified as having the lowest validation loss metric across all variants (i.e., MSE for regression, and SCCE for classification). We omit the complete training results across all models for brevity, instead concisely listing the best models and their hyperparameters in Table I. Specifically, we found **FoT model 9**, **ViT model 37**, **regression FuT model 20**, **classifier FuT model 43**, and **multi-task FuT model 42** as the best. The train/val/test performance for these models across all epochs are shown in Fig. 9. Likewise, their train/val/test metrics are shown visually in Fig. 10, and tabularly in Tables IIa and IIb. Further, while raw performance is important, computational complexity should also be taken into account, especially in IoT environments where energy and compute resources are at a premium. To finalize the comparison between models we therefore also consider their size (in number of parameters). The total sizes of these best models are shown in Table III.

TABLE I  
HYPERPARAMETERS OF THE TOP-PERFORMING MODELS FOR EACH TASK. UNLISTED VALUES INDICATE THE ASSOCIATED PARAMETER IS NOT USED FOR THE MODEL.

Model	$P_{\text{drop}}$	$k$	$D_e$	$D_{\text{ff}}$	$E$	$h$	$(H_p, W_p)$	$D_{\text{fusion}}$
FoT 9	0.1	5		512	6	8		
ViT 37	0.3		32	256	6	8	(6,6)	
Regression FuT 20	0.3	5	32	256	3	8	(6,6)	8
Classifier FuT 43	0.3	10	32	256	6	8	(6,6)	
Multi-Task FuT 42	0.3	5	32	256	6	8	(6,6)	16

Consider the performance of the regression models in Table IIa, Fig. 9a, and Figs. 10a and 10b. First, we see that our proposed FoT model 9 exhibits slightly better training, validation, and testing performance compared to the baseline LSTM. Specifically, FuT model 9 achieves train/val/test MSE 0.9939/0.8630/0.5057 and MAE 0.5258/0.4956/0.4668, whereas the LSTM achieves MSE 1.0078/0.8728/0.5044 and MAE 0.5284/0.4957/0.4745. Second, we see that our proposed single-task FuT regression model 20 outperforms the previous models in all metrics, while also exhibiting the highest overall validation scores, with MSE

<sup>4</sup>[https://www.tensorflow.org/api\\_docs/python/tf/keras/applications/inception\\_v3/InceptionV3](https://www.tensorflow.org/api_docs/python/tf/keras/applications/inception_v3/InceptionV3)

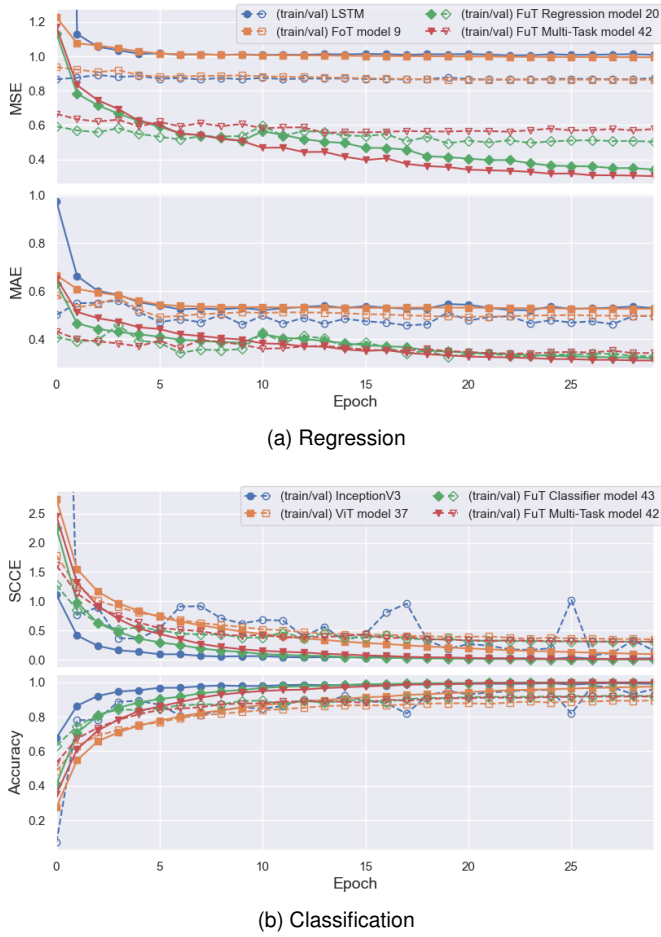


Fig. 9. Training and validation performance of best models on (a) classification, and (b) regression tasks.

0.3414/0.5031/0.5999 and MAE 0.3194/0.3270/0.3632. Finally, we see that our proposed multi-task FuT model 42 outperforms all other models in terms of training and test performance, with train/val/test MSE 0.3031/0.5767/0.4734 and MAE 0.3092/0.3405/0.3554. In addition, the lack of plateau in its training and validation performance in Fig. 9a indicates that increased training could further improve the model.

Next, consider the performance of the classification models in Table IIb, Fig. 9b, and Figs. 10c and 10d. Here we see much more variation between training, validation, and testing SCCE loss and accuracy metrics. First, the InceptionV3 model exhibits the best validation and test scores, with SCCE 0.0276/0.1581/0.1490 and accuracy 0.9912/0.9606/0.9615. However, its convergence in Fig. 9b is much more unstable starting around epoch 5. Second, we see that ViT model 37 learns the training set rather well, but performs the worst in validation and test metrics, with SCCE 0.0977/0.3499/0.3307 and accuracy 0.9750/0.8936/0.8978. Lastly, we see our proposed single-task FuT classifier model 43 (SCCE 0.0064/0.3112/0.3057, accuracy 0.9994/0.9202/0.9192) and multi-task FuT model 42 (SCCE 0.0135/0.3108/0.2985, accuracy 0.9987/0.9176/0.9166) exhibit very similar performance.

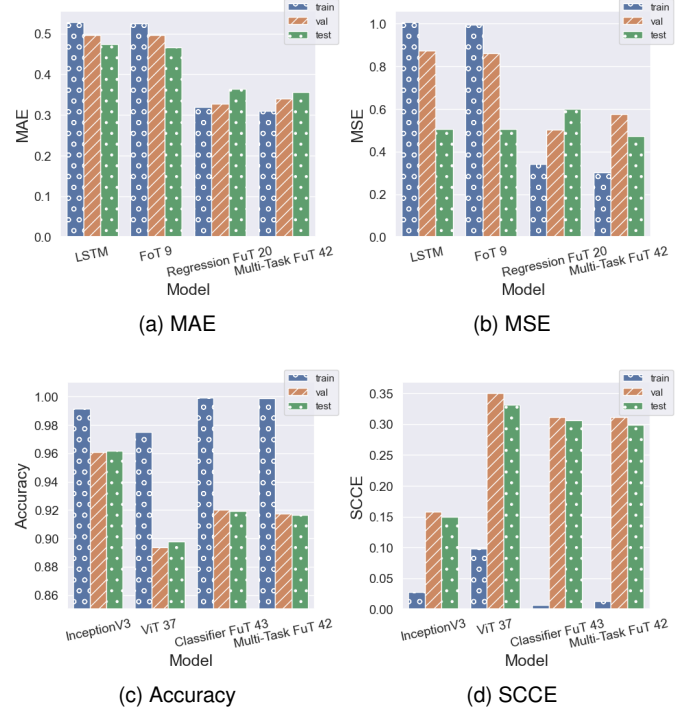


Fig. 10. Comparison between best model metrics for regression (a) MAE and (b) MSE, and classification (c) Accuracy and (d) SCCE.

TABLE II  
PERFORMANCE OF BEST TRAINED MODELS ON (A) REGRESSION, AND (B) CLASSIFICATION TASKS. BEST METRICS IN EACH COLUMN ARE HIGHLIGHTED IN **BOLD**.

(a) Regression						
Model	MSE			MAE		
	<i>train</i>	<i>val</i>	<i>test</i>	<i>train</i>	<i>val</i>	<i>test</i>
LSTM	1.0078	0.8728	0.5044	0.5284	0.4957	0.4745
FoT 9	0.9939	0.8630	0.5057	0.5258	0.4956	0.4668
Regression FuT 20	0.3414	<b>0.5031</b>	0.5999	0.3194	<b>0.3270</b>	0.3632
Multi-Task FuT 42	<b>0.3031</b>	0.5767	<b>0.4734</b>	<b>0.3092</b>	0.3405	<b>0.3554</b>

(b) Classification						
Model	SCCE			Accuracy		
	<i>train</i>	<i>val</i>	<i>test</i>	<i>train</i>	<i>val</i>	<i>test</i>
InceptionV3	0.0276	<b>0.1581</b>	<b>0.1490</b>	0.9912	<b>0.9606</b>	<b>0.9615</b>
ViT 37	0.0977	0.3499	0.3307	0.9750	0.8936	0.8978
Classifier FuT 43	<b>0.0064</b>	0.3112	0.3057	<b>0.9994</b>	0.9202	0.9192
Multi-Task FuT 42	0.0135	0.3108	0.2985	0.9987	0.9176	0.9166

In addition, the convergence of all our proposed classifier models exhibits a plateau by epoch 30. This indicates that further training on the image dataset would likely not improve classification performance.

Next, consider the relationship between model size and overall performance for single-task learners with and without data fusion. Here we see that the FuT regression model 20 has 47,288 *fewer* parameters compared to FoT model 9, and 8,071,256 *fewer* parameters than the baseline LSTM, while exhibiting significantly better performance. In contrast, the FuT classification model 43 has 222,504 *more* parameters than

TABLE III

SIZE COMPARISON OF BEST MODELS PER INPUT AND TASK TYPES VIA TOTAL NUMBER OF PARAMETERS. HERE WE ALSO SHOW THE SIZE OF COMBINED SINGLE-TASK MODELS FOR COMPARISON WITH MULTI-TASK VARIANTS.

Input Type	Task Type	Model	Parameters	
			<i>Individual</i>	<i>Combined</i>
Single-input	Single-task	LSTM	8,191,298	30,071,944
		InceptionV3	21,880,646	
		FoT 9	167,330	476,712
		ViT 37	309,382	
Multi-input	Single-task	Regression FuT 20	120,042	651,928
		Classifier FuT 43	531,886	
	Multi-task	FuT 42	<b>428,488</b>	-

ViT model 37 and has similar performance. This indicates that, while not guaranteed, data fusion can enhance performance, but can also come at the cost of increased complexity. However, comparing with the baseline InceptionV3, we see a dramatic reduction of 21,571,264 fewer parameters. As discussed in Section IV-C, the baseline InceptionV3 indeed has better performance than ViT, however, the boost is marginal when also comparing the memory and computational complexities introduced by such a large increase in model size.

Finally, consider the overall performance of multi-task learners with combined single-task variants. To perform multiple tasks using single fusion models, we must combine FuT regression model 20 and classification model 43. However, doing so requires a total of  $120,042 + 531,886 = 651,928$  parameters. If we then compare the results of multi-task FuT model 42 we see that equivalent performance can be achieved with only 428,488 parameters (a reduction of 223,440). If we were to combine the simpler single-input single-task FoT and ViT models, totaling  $309,382 + 167,330 = 476,712$  parameters, multi-task FuT model 42 is still smaller (reducing the size by 48,224). Further, multi-task FuT model 42 is significantly smaller than the two baseline LSTM and InceptionV3 models combined, totaling  $8,191,298 + 21,880,646 = 30,071,944$  parameters. This reduction in model size is significant for two reasons. First, the smaller size requires less computational resources for inference, thereby making deployment more viable on IoT devices. Second, it also reduces the complexity of having two separate models, which further reduces memory overhead, and also reduces deployment costs, as one multi-task IoT device can do the job of two single-task variants. These boons in performance, efficiency, and cost therefore establish the multi-task data fusion architecture as the prime candidate for deployment in smart city environments.

## V. CONCLUSION

In this paper, we have provided several AI designs based on pure-encoder Transformer architectures for use in S&CC environments. We showed that pure-encoder Transformers serve as a viable baseline for single-task learning models, and demonstrated their capability on independent supervised multivariate time-series regression and computer vision classification tasks. We enhanced our proposed single-task AI system design by

leveraging the fusion of the aforementioned heterogeneous datasets as input, and showed that this fusion can improve learning over single-input variants. We further extended the fusion architecture with custom output task heads to facilitate heterogeneous multi-task learning. The flexibility offered by these custom heads allows our proposed architecture to support virtually any task, and any combination of tasks desired. We showed through extensive experimentation that our proposed multi-input multi-output enhancement either maintains or exceeds the performance capabilities of both single-task variants and non-Transformer baselines, while also reducing its memory footprint and computational overhead. Hence, we have demonstrated that our proposed next-generation multi-task Transformer-based AI system is viable for deployment in smart city environments. It can successfully learn to perform unique multivariate regression of time-series meteorological features, while concurrently identifying the onset of fungal diseases through visual feature extraction. Moreover, it performs these heterogeneous tasks using a fusion of both static images and multivariate time-series data. Indeed, this flexibility to support diverse feature sets from heterogeneous IoT data sources, while also learning a variety of tasks in parallel, shows that our system can bolster sustainable urban development practices, and, in particular, foster the growth of S&CCs.

## REFERENCES

- [1] United Nations, "World Urbanization Prospects The 2018 Revision," United Nations, Tech. Rep., 2018. [Online]. Available: <https://population.un.org/wup/Publications/Files/WUP2018-Report.pdf>.
- [2] A. Vaswani, N. Shazeer, N. Parmar, J. Uszkoreit, L. Jones, A. N. Gomez, L. Kaiser, and I. Polosukhin, "Attention Is All You Need," Jun. 2017. [Online]. Available: <http://arxiv.org/abs/1706.03762>.
- [3] B. Lim, S. O. Arik, N. Loeff, and T. Pfister, "Temporal Fusion Transformers for Interpretable Multi-horizon Time Series Forecasting," *International Journal of Forecasting*, vol. 37, no. 4, Dec. 2019. [Online]. Available: <http://arxiv.org/abs/1912.09363>.
- [4] H. Zhou, S. Zhang, J. Peng, S. Zhang, J. Li, H. Xiong, and W. Zhang, "Informers: Beyond Efficient Transformer for Long Sequence Time-Series Forecasting," Dec. 2020. [Online]. Available: <http://arxiv.org/abs/2012.07436>.
- [5] N. Wu, B. Green, X. Ben, and S. O'Banion, "Deep Transformer Models for Time Series Forecasting: The Influenza Prevalence Case," Jan. 2020. [Online]. Available: <http://arxiv.org/abs/2001.08317>.
- [6] G. Zerveas, S. Jayaraman, D. Patel, A. Bhamidipaty, and C. Eickhoff, "A Transformer-based Framework for Multivariate Time Series Representation Learning," Oct. 2020. [Online]. Available: <http://arxiv.org/abs/2010.02803>.
- [7] J. Grigsby, Z. Wang, and Y. Qi, "Long-Range Transformers for Dynamic Spatiotemporal Forecasting," Sep. 2021. [Online]. Available: <http://arxiv.org/abs/2109.12218>.
- [8] A. Dosovitskiy, L. Beyer, A. Kolesnikov, D. Weissenborn, X. Zhai, T. Unterthiner, M. Dehghani, M. Minderer, G. Heigold, S. Gelly, J. Uszkoreit, and N. Houlsby, "An Image is Worth 16x16 Words: Transformers for Image Recognition at Scale," *The International Conference on Learning Representations*, Oct. 2020. [Online]. Available: <http://arxiv.org/abs/2010.11929>.
- [9] R. Reedha, E. Dericquebourg, R. Canals, and A. Hafiane, "Transformer Neural Network for Weed and Crop Classification of High Resolution UAV Images," *Remote Sensing*, vol. 14, no. 3, p. 592, Jan. 2022, ISSN: 2072-4292. DOI: 10.3390/rs14030592. [Online]. Available: <https://www.mdpi.com/2072-4292/14/3/592>.
- [10] H.-T. Thai, N.-Y. Tran-Van, and K.-H. Le, "Artificial Cognition for Early Leaf Disease Detection using Vision Transformers," in *2021 International Conference on Advanced Technologies for Communications (ATC)*, vol. 2021-October, IEEE, Oct. 2021, pp. 33–38, ISBN: 978-1-6654-3379-2. DOI: 10.1109/ATC52653.2021.9598303. [Online]. Available: <https://ieeexplore.ieee.org/document/9598303/>.

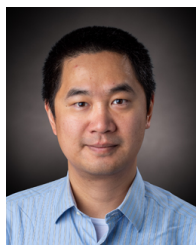
- [11] A. Prakash, K. Chitta, and A. Geiger, "Multi-Modal Fusion Transformer for End-to-End Autonomous Driving," Apr. 2021. [Online]. Available: <http://arxiv.org/abs/2104.09224>.
- [12] R. Hu and A. Singh, "UniT: Multimodal Multitask Learning with a Unified Transformer," Feb. 2021. [Online]. Available: <http://arxiv.org/abs/2102.10772>.
- [13] A. Zeng, M. Chen, L. Zhang, and Q. Xu, "Are Transformers Effective for Time Series Forecasting?," May 2022. [Online]. Available: <http://arxiv.org/abs/2205.13504>.
- [14] Y. Wang, R. Huang, S. Song, Z. Huang, and G. Huang, "Not All Images are Worth 16x16 Words: Dynamic Transformers for Efficient Image Recognition," *NeurIPS*, no. NeurIPS, pp. 1–16, May 2021. [Online]. Available: <http://arxiv.org/abs/2105.15075>.
- [15] A. Kolesnikov, L. Beyer, X. Zhai, J. Puigcerver, J. Yung, S. Gelly, and N. Houlsby, "Big Transfer (BiT): General Visual Representation Learning," Dec. 2019. [Online]. Available: <http://arxiv.org/abs/1912.11370>.
- [16] *Modernizing cities via smart garden alleys with application in makassar city (award # 2025377)*. [Online]. Available: [https://www.nsf.gov/awardsearch/showAward?AWD\\_ID=2025377&HistoricalAwards=false](https://www.nsf.gov/awardsearch/showAward?AWD_ID=2025377&HistoricalAwards=false).
- [17] J. Devlin, M.-W. Chang, K. Lee, and K. Toutanova, "BERT: Pre-training of Deep Bidirectional Transformers for Language Understanding," Oct. 2018. [Online]. Available: <http://arxiv.org/abs/1810.04805>.
- [18] Z. Yang, Z. Dai, Y. Yang, J. Carbonell, R. Salakhutdinov, and Q. V. Le, "XLNet: Generalized Autoregressive Pretraining for Language Understanding," Jun. 2019. [Online]. Available: <http://arxiv.org/abs/1906.08237>.
- [19] T. B. Brown, B. Mann, N. Ryder, M. Subbiah, J. Kaplan, P. Dhariwal, A. Neelakantan, P. Shyam, G. Sastry, A. Askell, S. Agarwal, A. Herbert-Voss, G. Krueger, T. Henighan, R. Child, A. Ramesh, D. M. Ziegler, J. Wu, C. Winter, C. Hesse, M. Chen, E. Sigler, M. Litwin, S. Gray, B. Chess, J. Clark, C. Berner, S. McCandlish, A. Radford, I. Sutskever, and D. Amodei, "Language Models are Few-Shot Learners," May 2020. [Online]. Available: <http://arxiv.org/abs/2005.14165>.
- [20] S. M. Kazemi, R. Goel, S. Eghbali, J. Ramanan, J. Sahota, S. Thakur, S. Wu, C. Smyth, P. Poupart, and M. Brubaker, "Time2Vec: Learning a Vector Representation of Time," Jul. 2019. [Online]. Available: <http://arxiv.org/abs/1907.05321>.
- [21] Y. Lecun, L. Bottou, Y. Bengio, and P. Haffner, "Gradient-based learning applied to document recognition," *Proceedings of the IEEE*, vol. 86, no. 11, pp. 2278–2324, 1998, ISSN: 00189219. DOI: 10.1109/5.726791. [Online]. Available: <http://ieeexplore.ieee.org/document/726791>.
- [22] A. Krizhevsky, I. Sutskever, and G. E. Hinton, "ImageNet Classification with Deep Convolutional Neural Networks," in *Advances in Neural Information Processing Systems*, F. Pereira, C. J. C. Burges, L. Bottou, and K. Q. Weinberger, Eds., vol. 25, Curran Associates, Inc., 2012. [Online]. Available: <https://proceedings.neurips.cc/paper/2012/file/c399862d3b9d6b76c8436e924a68c45b-Paper.pdf>.
- [23] A. Farahani, B. Pourshojae, K. Rasheed, and H. R. Arabnia, "A Concise Review of Transfer Learning," Apr. 2021. [Online]. Available: <http://arxiv.org/abs/2104.02144>.
- [24] S. Chen, *Beijing PM2.5 Data*, UCI Machine Learning Repository, 2017. [Online]. Available: <https://archive-beta.ics.uci.edu/ml/datasets/beijing+pm2+5+data>.
- [25] D. P. Hughes and M. Salathe, "An open access repository of images on plant health to enable the development of mobile disease diagnostics," Nov. 2015. [Online]. Available: <http://arxiv.org/abs/1511.08060>.
- [26] C. Szegedy, V. Vanhoucke, S. Ioffe, J. Shlens, and Z. Wojna, "Re-thinking the Inception Architecture for Computer Vision," Dec. 2015. [Online]. Available: <http://arxiv.org/abs/1512.00567>.
- [27] J. Deng, W. Dong, R. Socher, L.-J. Li, Kai Li, and Li Fei-Fei, "ImageNet: A large-scale hierarchical image database," in *2009 IEEE Conference on Computer Vision and Pattern Recognition*, IEEE, Jun. 2009, pp. 248–255, ISBN: 978-1-4244-3992-8. DOI: 10.1109/CVPR.2009.5206848. [Online]. Available: <https://ieeexplore.ieee.org/document/5206848/>.



**Alexander C. DeRieux** (Graduate Student Member, IEEE) received the B.S. degree in electrical engineering with honors and the B.S. degree in computer science with honors from Virginia Tech, Blacksburg, VA, USA, in 2016, and the M.S. degree in electrical engineering in 2022. He is currently a Ph.D. student in electrical engineering and Bradley Fellow at the Network sciEence, Wireless, and Security (NEWS) Laboratory in the Bradley Department of Electrical and Computer Engineering at Virginia Tech. His research interests include machine learning, quantum computing, quantum machine learning, quantum communications, and wireless networks.



**Walid Saad** (Fellow, IEEE) (S'07, M'10, SM'15, F'19) received his Ph.D degree from the University of Oslo in 2010. He is currently a Professor at the Department of Electrical and Computer Engineering at Virginia Tech, where he leads the Network sciEence, Wireless, and Security (NEWS) laboratory. He is also the Next-G Wireless research leader at Virginia Tech's Innovation Campus. His research interests include wireless networks (5G/6G/beyond), machine learning, game theory, security, unmanned aerial vehicles, semantic communications, cyber-physical systems, and network science. Dr. Saad is a Fellow of the IEEE. He was the author/co-author of eleven conference best paper awards. He is the recipient of the 2015 and 2022 Fred W. Ellersick Prize from the IEEE Communications Society, of the 2017 IEEE ComSoc Best Young Professional in Academia award, of the 2018 IEEE ComSoc Radio Communications Committee Early Achievement Award, and of the 2019 IEEE ComSoc Communication Theory Technical Committee. He was also a co-author of the 2019 and 2021 IEEE Communications Society Young Author Best Paper. He is the Editor-in-Chief for the IEEE Transactions on Machine Learning in Communications and Networking.



physical systems, and network science. Dr. Saad is a Fellow of the IEEE. He was the author/co-author of eleven conference best paper awards. He is the recipient of the 2015 and 2022 Fred W. Ellersick Prize from the IEEE Communications Society, of the 2017 IEEE ComSoc Best Young Professional in Academia award, of the 2018 IEEE ComSoc Radio Communications Committee Early Achievement Award, and of the 2019 IEEE ComSoc Communication Theory Technical Committee. He was also a co-author of the 2019 and 2021 IEEE Communications Society Young Author Best Paper. He is the Editor-in-Chief for the IEEE Transactions on Machine Learning in Communications and Networking.

**Wangda Zuo** is a Professor in Architectural Engineering and Mechanical Engineering, as well as Associate Director for Research at Global Building Network at Pennsylvania State University. Dr. Zuo also holds a joint appointment at the National Renewable Energy Laboratory (NREL). He is currently an Associate Editor of Journal of Solar Energy Engineering, and Fellow of International Building Performance Simulation Association. He is a major contributor to multiple open-source building and community energy modeling tools, including Mod-elica Buildings library and URBANopt.



related projects and 20 other projects, which some of them were/are funded by 17 international institutions.

**Rachmawan Budiarto** is a faculty member in Department of Nuclear Engineering and Engineering Physics, Director of Centre for Development of Sustainable Region (CDSR) in Centre for Energy Studies as well as a senior researcher at Center for Economic Democracy Studies, Universitas Gadjah Mada. He is a Greenship Professional of Green Building Council Indonesia. He is a member of International Committee of Indonesia Accreditation Board for Engineering Education (IABEE). He was/is involved in at least 81 sustainable energy



**Dr Eng. Mochamad Donny Koerniawan, ST, MT**

, lecturer and researcher in Building Technology Research Group within The School of Architecture Planning and Policy Development. Institut Teknologi Bandung, vice president of International Building Simulation Association, Indonesia Chapter; Green Associate and Member of Green Building Council Indonesia (GBCI); member of Association Green Building Expert Indonesia; Member of Indonesia Architect Institute. Highly experienced in green building research and development. Development of

Sustainable Region (CDSR) in Centre for Energy Studies.



**Dwi Novitasari** is a Ph.D. student at the Department of Electrical Engineering and Information Technology, Universitas Gadjah Mada. She is also a researcher at the Centre for Energy Studies and the Centre for Development of Sustainable Region (CDSR), Universitas Gadjah Mada. She was/is involved in national and international projects related to renewable energy, energy planning, energy transition, and sustainable energy. Currently, her research is about climate, land use, energy, and water nexus in power generation planning in Indonesia. She

also received the Canada-ASEAN Exchange Scholarship at the School of Sustainable Energy Engineering, Simon Fraser University.